Expanding the material palette for Selective Laser Sintering: two production techniques for spherical powders

N. Mys[a], A. Verberckmoes[b], L. Cardon[a]

[a]*Centre for Polymer and Material Technologies (CPMT), Faculty of Engineering and Architecture, Ghent University, Tech Lane Science Park – Campus A, Technologiepark Zwijnaarde 915, 9052 Zwijnaarde, Belgium*

[b]*INdustrial Catalysis and Adsorption Technology (INCAT), Faculty of Engineering and Architecture, Ghent University, Valentin Vaerwyckweg 1, 9000 Ghent, Belgium*

ABSTRACT: Selective laser sintering is a rapidly expanding field of the 3D printing concept. One stumbling block in the evolution of the technique is the limited range of materials available for processing with SLS making the application window rather small. This article aims at identifying two processing methods to create spherical powders as alternative techniques to the industrially used cryogenic milling. To this end, both a semi-crystalline polymer, syndiotactic polystyrene, and an amorphous polymer, polysulfone, are tested by processing them from pellet form to spherical powders using a spray drying technique and a rotor milling technique. Both methods are tested on their efficiency in producing suitable feed material for SLS based on morphology, size and flowability through SEM analyses and Hausner Ratio measurements. The powders are tested on the change in their intrinsic and extrinsic properties due to processing through GPC and DSC measurements.

1 INTRODUCTION

Additive manufacturing is an umbrella term among which several 3D techniques house. It is the process of turning a digital design into a three-dimensional object, a fast and convenient way of making functional prototypes or actual finished products. These technologies allow tailor-made products with higher geometrical complexity than possible when using conventional manufacturing techniques like injection molding. Selective laser sintering (SLS) is such a form of 3D printing in which the heat produced by a CO_2-laser is used to selectively fuse precise areas in a powder bed to form the three-dimensional object in a layerwise fashion. As the surrounding powder acts as support structure, no supports are needed allowing for more intricate designs to be produced. In this way, production costs can be lowered and the surrounding powders can be easily recycled making this technique interesting from an economical point of view.

Brought to life by the hands of Carl Deckard and his engineering professor Joe Beaman at the University of Texas, it was initially used as a rapid prototyping technique. In the last decades however, this technique has undergone a shift from rapid prototyping (RP) to the production of actual end-use products (Tiwari et al. 2015; Vasquez et al. 2014). This shift to finished products has ensured a more stringent focus on the material properties of the finished product in terms of its functionality. Attention has to be drawn to the mechanical, thermal or chemical properties depending of the use of the product. As a result, there is a pressing need to expand the material range in order to account for these new product demands.

Nowadays mainly polyamides are used (Zhou et al. 2013; Goodridge et al. 2010; Wegner et al. 2015; Bai et al. 2012; Drummer et al. 2015; Athreya et al. 2010) limiting the product applications to the properties of this polymer class. In more recent years, other materials have been introduced for processing among which poly(aryl-ether-ether-ketones) (PAEK, PEEK, PEKK) (Schmidt et al. 2007; Drummer et al. 2010; Pohle et al. 2007), polystyrene (PS) (Strobbe et al. 2016) polycarbonate (PC) (Berzins et al. 1996; Vasquez et al. 2014; Ho et al. 1999; Kruth et al. 2008) and thermoplastic elastomers as TPU (Dadbakhsh et al. 2016). It is important that these novel materials differ in properties of the usual materials in order to increase the possible applications for the SLS technique. Nevertheless, there is still a large discrepancy in the amount of material available for SLS versus the tens of thousands material grades available for injection molding. As these grades often do not exist in powder form but in pellet or droplet size they are not directly usable for processing through SLS. Transforming these materials to a suitable powder form that can be used as feed material for SLS can prove advantageous for its material palette. The particle size and morphology play a vital role in both the processing ability and the final characteristics of the part. Goodridge et al. (Goodridge et al. 2012) has defined the ideal particle size in the 45-90 µm range in order to optimize packing density of the powders without electrostatic buildup or risk of too much porosity. Particles should moreover be of spherical morphology and in the absence of any sharp features that could hamper the flow character

of the powders. This cannot be achieved using the conventional methods like cryogenic milling (Bai et al. 2000; Jonna & Lyons 2005; Goodridge et al. 2012) as particles are often angular and rough in shape causing a rough powder bed and inferior finish of the sintered part (Ziegelmeier et al. 2015).

This article aims at identifying two techniques suitable in producing powders that fulfill the requirements as feed material for SLS. In this regard, a physicochemical technique called spray drying and a mechanical technique called rotor milling are verified as powder production techniques starting from the commercial pellet form. The powders are characterized on their intrinsic and extrinsic properties through the use of Scanning Electron Microscopy (SEM), Differential Scanning Calorimetry (DSC) and Hausner Ratio (HR). This to ascertain if any changes have occurred in the polymer properties due to the processing method as well as to see if the produced powders fit the criteria as build material for SLS. Further tests regarding, Thermogravimetric Analysis (TGA), FIB-SEM density assesment and Gel Permease Chromatography (GPC) can be found in other works (Mys 2017; Mys, Van De Sande, et al. 2016; Mys, Verberckmoes, et al. 2016).

2 MATERIALS AND METHODS

2.1 *Materials*

Polysulphone Udel P-1700 was provided by Solvay in the form of pellets and was used as-received. The pellets were dissolved in N,N-Dimethylformamide (DMF, purity 99+ %). sPS XAREC S90Z was provided by Idemitsu Chemicals Europe, unfilled, in the form of pellets and was used as-received. The pellets were dissolved in m-xylene (purity 98%).

2.2 *Methods*

2.2.1 *Spray drying*

Spray drying was performed on a Buchi B290 equipped with a two-fluid nebulizer connected to pressurized air. The nozzle orifice size was 2,0 mm. The aspirator ran at a maximum air velocity of 40 m³/h. The heater inlet temperature, temperature of solution, solution feeding rate and gas flow rate were fixed factors in this article. The optimization of the morphology of the particles is elaborately described elsewhere (Mys 2017). For this purpose a fixed set of parameters is used based on previous obtained results.

In the case of PSU, a solution of 12 wt% in DMF was heated to 150 °C and fed to the nozzle at a feed rate of 7,4 mL/min. The prepared solution was heated to decrease the solution viscosity and hence increase the diffusion rate of the solutes during drying. The heated solution was then atomized by the two-fluid nozzle using a gas flow rate of 439 L/h into the drying chamber where the droplets were dried by the use of dry air at 210 °C.

For sPS, a solution of 2,5 wt% in m-xylene was heated to 150 °C and fed to the nozzle using fluoroelastomer tubes at a feed rate of 20 mL/min. The polymer solution was heated to lower the solution viscosity for atomization and avoid crystallization of the sPS in solution (Woo et al. 2001). As a measure to further prevent this gelation/crystallization phenomenon the tubes were preheated by spraying warm solvent prior to spray drying the polymer solution. The heated solution was thereafter atomized using the two-fluid atomizer into the drying chamber using a gas flow rate of 439 L/h. Particles were subsequently dried by a heating gas (pressurized air) which was heated at 200 °C. The resulting powder was sieved off using a cyclone system and investigated.

2.2.2 *Rotor milling*

Rotor milling was performed on a Fritsch Pulverisette 14 rotor mill to pulverize the polysulfone ans syndiotactic polystyrene pellets by a three-step communition process. In a first step the pellets were pulverized to a coarse powder using a sieve with mesh size of 500 μm. In a second and third refinement step the coarse powder is further pulverized to a fine powder and sieved at 120 μm and 80 μm subsequently. A 12 ribbed rotor blade was used at 15000 RPM to achieve pulverisation. The resulting powder was sieved and isolated using a cyclone system. During the milling process the rotor mill was cooled by air at room temperature using an aspirator connected to the cyclone system.

2.2.3 *Particle Size assessment (PSD)*

The morphology of the produced particles was investigated using a scanning electron microscopy (JEOL JSM-7600F) at low voltage (2kV) and working distance of 8mm. Samples were sputtered shortly with gold using a BAL-TEC SCD 005 Sputter Coater at 25mA. Obtained micrographs were then analyzed using the software program Image J and further investigated using the statistical program SPSS.

2.2.4 *Morphology assessment*

The morphology of the particles was assessed based on their shape (sphericity) as well as their roundness. Both have been found to impact flow characteristics of powder bulk material substantially (Bodhmage 2006). Visual patterns are most commonly used to determine the degree of roundness and sphericity (Grabowski & Wilanowicz 2008). The Powers' pattern (Figure 1, (Powers 1982)) is one of the most popular patterns which connect roundness and sphericity. The chart offers a quick and easy way to process and classify the samples and gives an idea of the suitability of the samples for laser sintering. The particles in this paper were characterized using their maximum diameter (case C in Figure 2). For particle morphology assessment a manual point count based

on the ASTM E562M standard method in combination with the Powers' pattern depicted in Figure 2 was used. Particles graded with values scaling them inside the red box were considered of apt sphericity and roundness.

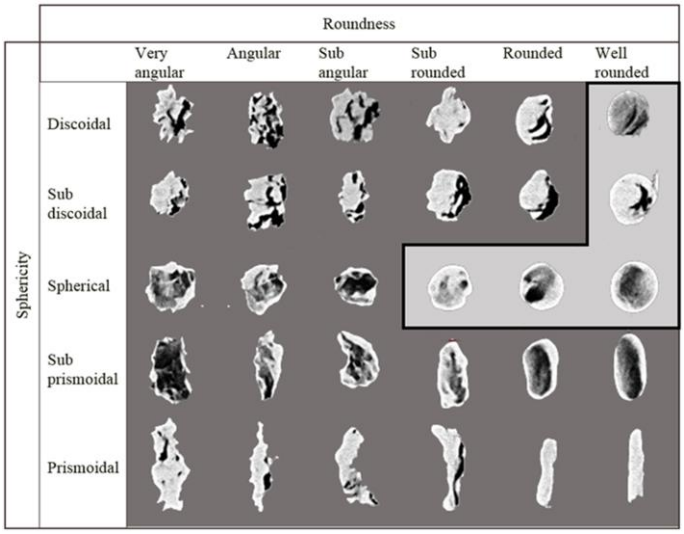

Figure 1: Powers' Pattern for estimation of morphology of produced particles. Particles in the light grey area are considered apt for SLS. Figure derived from (Powers 1982)

2.2.5 *Hausner Ratio (HR)*

The Hausner Ratio describes the ratio of the tapped and bulk density of a powder and classifies the powders flowability (Ziegelmeier et al. n.d.; Schmid et al. 2013). The HR scale can be subdivided into three main regions (Barbosa-Cánovas et al. 2005):

- HR < 1,25 : which are easily fluidized
- 1,25 < HR < 1,4 : decreasing fluidization
- HR > 1,4 : fluidization problems

The HR test was performed by gravimetrically measuring the densities of the powder at ambient conditions using a graduated cylinder and powder funnel. After measuring the bulk density the powder was subjected to a sequence of taps by placing the cylinder on the baseplate of a Retsch Vibratory Sieve Shaker AS 200 digit for 60 seconds at 60% of its maximal amplitude. Afterwards the volume was measured again to determine the tapped density. To increase its statistical outcome, each powder sample was measured over 10 times (using fresh powder every time) as the HR is highly dependent on the analyst due to the tapping of the powder samples and determination of the volume in the graduated cylinder. The Hausner ratio was calculated as follows:

$$HR = \rho_{tapped} / \rho_{bulk} \quad (1)$$

where ρ_{bulk} and ρ_{tapped} are the freely settled bulk density of the powder and the tapped density of the powder in which the powder is tapped until no further changes occur. In this article the HR of the rotor milled samples could only be calculated as the spray drying and ball milling experiments were conducted on lab scale and did not produce enough quantity to allow HR to be determined.

2.2.1 *DSC measurements*

The thermal properties of the produced powders were analyzed using a Netzsch DSC 204F1 under nitrogen atmosphere. Samples were contained in an open Aluminum pan and referenced against an empty open Aluminum pan. A heating rate of 10 °C/min was used to heat the DSC to 450 °C or 290 °C respectively for PSU and sPS. This was done to determine the effects of degradation and thermal history imparted during processing. An isotherm was upheld at these temperatures to ensure all orientations, crystalline or otherwise, were gone. A second heating run under the same conditions was performed to determine if any change in thermal properties had occurred. A baseline subtraction was done to correct for any slope or variation in heat transfer effects by performing the same measurement with an empty pan both in the reference and sample position and then subtracting the resultant curve.

3 RESULTS

3.1.1 *Particle size assessment (PSD)*

Figure 2 depicts the SEM micrographs of the processed samples through rotor milling (above) and spray drying (below). The corresponding PSD analysis is presented next to it with the data summarized in Table 1. A large difference in mean particle size is visible between the semi-crystalline sPS and the amorphous PSU which can be directly correlated with their maximum solubility in their respective solvent. Whereas PSU could be atomized at 12 wt%, sPS could only be sprayed successfully at 2,5 wt% which is reflected directly in the smaller particle size due to the atomization of more diluted solutions. PSU displayed a mean particle size of 26,10 µm and a standard deviation of 12,80 µm while sPS showed a mean particle size of 6,60 µm with 6,90 µm standard deviation.

Contrariwise to the spray drying process, rotor milling achieves particle sizes more in range of the required diameters. Both for sPS and PSU a particle size of 49,22 ± 15,61 µm and 51,80 ±15,20 µm respectively are achieved.

3.1.1 *Particle morphology assessment*

Evaluation of the particle morphology via the manual point count method described above is represented in Table 1 and Figure 2. The results reveal the spray drying technique to be an excellent technique for producing particles with a smooth surface and high sphericity. Both sPS and PSU have a high number of particles fulfilling the morphology requirements as-

sessed via the Powers' table. Nevertheless, a small part of the particles displays either collapsed or string-like structures. The latter can be caused by too high viscosity of the solution causing bad jetting behavior while the former can be ascribed to the formation of a skin layer in the drying process of the atomized solution ((Mys, Van De Sande, et al. 2016; Vehring et al. 2007)). During the drying process, the solvent in the atomized solution starts to evaporate. Due to the low diffusion rate of polymers the solute starts to enrich at the droplet surface causing a concentration gradient to occur. As evaporation continues, saturation will occur at the droplet surface and a skin or shell will be formed. Depending on the rate of evaporation this shell can be mechanically stable enough to sustain itself or collapse with the receiving droplet surface resulting in the collapsed structures. As sPS could only be dissolved in a lower weight percentage, it is more prone to form thinner shells causing a higher number of collapsed structures which is reflected in the results in Table 1.

Besides spray drying, the rotor milling technique is also capable of producing particles of some degree of sphericity. Here, the particles impact against a high speed rotating rotor blade causing the material to deform at the contact area. The kinetic energy of the rotor is in this way transferred (partly) to the material and, as elastic stress reaches a critical level, causes the material to deform and ultimately to break. After this initial fragmentation the particles are driven outwards under influence of the centrifugal force and experience extra shear forces between the rotor and inset sieve ring causing further fragmentation and the rounding of the particles by the rotating motion of the blade. This rounding of the particles is more outspoken in PSU than with the more brittle sPS which tends to fragment easier. The mechanical processing of the polymer material gives rounded off particles which are more deviant from the ideal spherical particles and have a rougher surface causing less of the particles to fit the Powers' requirements (see Table 1).

3.1.2 *Hausner Ratio Measurements*

The results of the density and Hausner ratio measurements are depicted in Figure 3. PSU and sPS both display different behavior when going through the different milling steps. Although both materials reach the limit of good powder flowability in their final form, PSU displays a better packing density than sPS. An explanation could lie in the differences of dominating adhesive forces in the powder bulk of sPS together with their more edgy, less rounded form of the particles which hamper flowability. A similar effect was noticed by Ziegelmeier et.al.

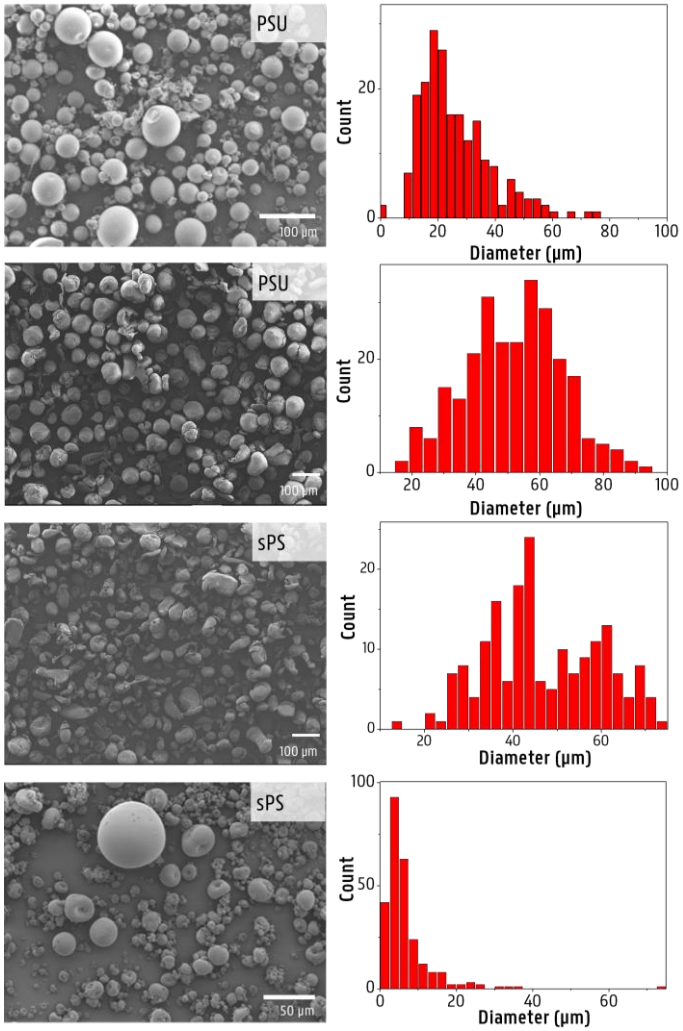

Figure 2: SEM micrographs of spray dried (upper micrograph) and rotor milled (lower micrograph) samples of PSU and sPS

Table 1: Particle Size Distribution of the rotor milled and spray dried particles with the assessment of morphology according to the Powers' table

	Particle size (µm)	Morphology (% apt particles)
	Rotor Milling	
PSU	51,80 ± 15,20	39,0
sPS	49,22 ± 15,61	26,8
	Spray Drying	
PSU	26,1 ± 12,8	71,0
sPS	6,6 ± 6,9	56,7

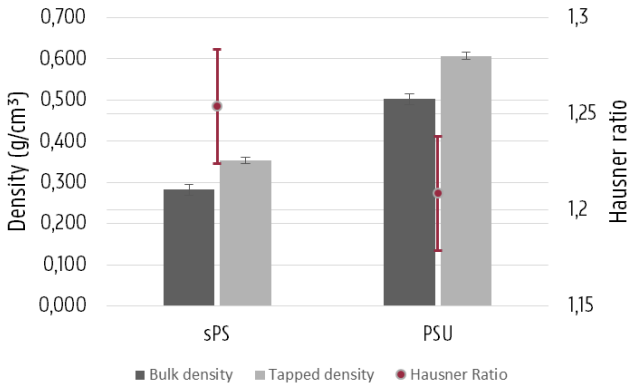

Figure 3: The bulk and tapped density of the PSU and sPS powders with the calculated values for the Hausner Ratio

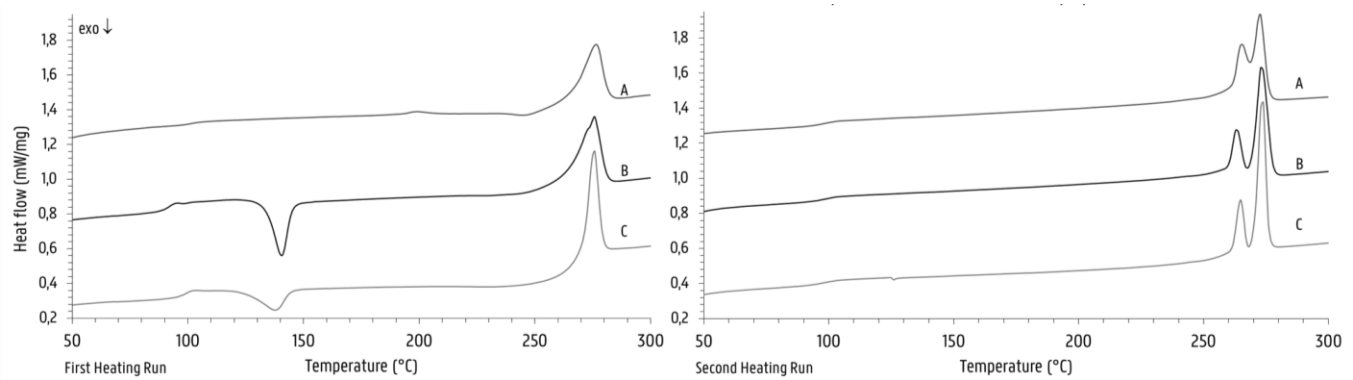

Figure 4: DSC run of sPS in first (left) and second (right) heating run. (A) The virgin polymer, unprocessed, (B) the spray dried sample and (C) the rotor milled sample

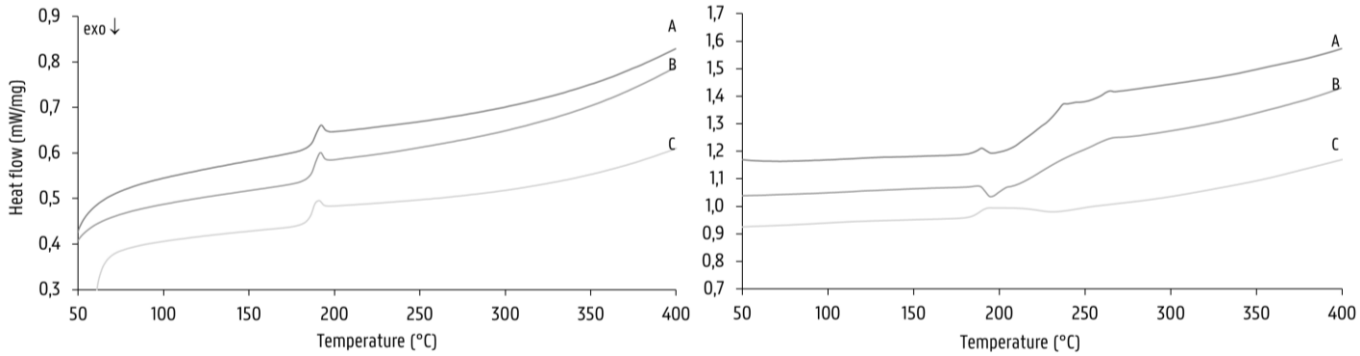

Figure 5: DSC run of PSU in first (left) and second (right) heating run. (A) the spray dried sample, (B) the rotor milled sample and (C) The virgin polymer, unprocessed

(Ziegelmeier et al. n.d.) in the comparison of the HR of different TPU powders and concluded that changes in the dominating adhesive forces in the powder bulk were culpable. As particle size decreases these adhesive forces would gain influence and could cause agglomeration hindering packing efficiency and effectively lower particle density.

3.1.3 *DSC measurements*

The thermal history imparted on the powders by each of the processing methods was investigated using the first heating curve (Figure 4 and Figure 5, left graph). This heating run could be especially helpful in setting the parameters for laser sintering for which these powders are intended. To explore the reversibility of the structural changes imparted by the processing techniques a second heating run is explored (Figure 4 and Figure 5, right graph).

Syndiotactic polystyrene is a polymorphic semi-crystalline polymer. Four crystal types (α, β, γ and δ) with sub-modifications for both the α- and β-form exist depending on if the material is thermal (α- and β-form) or solvent (γ and δ-form) treated. E. M. Woo et al. (Woo et al. 2001) did an extensive review on the complex polymorphism of syndiotactic polystyrene explaining the thermal profiles of the more common α- and β-forms with their trans-planar conformation and helical conformation associated with the γ and δ-forms. The polymorph behavior of sPS described in this paper is reflected in the first heating run of the unprocessed material by a broad endothermic peak at 277 °C (Figure 4, left, A). Following the same heating rates as described by Woo et al. (Woo et al. 2001) the polymer was cooled down stimulating α”-crystal formation. This type of crystal structure is confirmed in the second heating run by the dual melting peak at 265 °C and 272 °C, identified as P-II and P-IV, and a minor endothermic peak at 246 °C, labeled as $P_{a,\alpha}$, attributed to the annealing effect of the cooling rate on the α”-type crystal.

Upon processing of the sPS significant changes in thermal behavior occur. In the case of spray drying (Figure 4, B) a relatively large cold crystallization peak becomes apparent at 139 °C. This can be explained when looking at the spray drying process: a large temperature gradient exists between the drying chamber at high temperature and the collection vessel in which the microspheres are collected at practically ambient temperature. Partial quenching is believed to occur which is reflected by cold crystallization upon the first thermal run. The glass transition is found at 92 °C but increases back to 98,9 °C in the second thermal run suggesting no severe degradation to have occurred during processing. The broad melting peak at 275 °C also deviates a little from the polymorphic profile as seen with untreated sPS by the appearance of a small shoulder: a partial preferred crystallization from solvent due to the thermal treatments upon processing is said to occur. Upon the second thermal run the thermal history of the processing technique is swept away and a clear α”-structure is recovered evidenced by the dual

melting peaks at 263 °C and 273 °C. The initial decrease in crystallinity can hence be explained by the fast cooling of the particles upon consolidating in the drying chamber and subsequent cooling in the collecting chamber resulting in a more amorphous sPS than the virgin material.

When looking at the mechanical processing techniques a similar trend of amorphization can be seen. In the case of rotor milling an exothermic peak is detected at 132 °C upon heating. Here, the cold crystallization peak at 132 °C can be attributed to amorphization due to the mechanical treatment. This strain-induced amorphization of the crystalline regions is also known as decrystallization or disaggregation and is explained by D. Raabe et al. (Raabe et al. 2004) as sheared crystalline lamellae that break apart into sets of crystalline blocks with severe lattice defects, also called mechanical melting. The second DSC run reveals a return of the dual melting peaks though a larger incision is visible between the two characteristic peaks. Though the milling process only takes up a fraction of seconds, the powders are subjected to multiple treatments to further reduce the particle size which could have a cumulative effect on degradation behavior. Finally, the glass transition temperature was measured at 95,7 °C, in close agreement to the unprocessed sample

PSU is an amorphous polymer leading to expect no change in the baseline of the thermogram except for the glass transition temperature. However, as is visible in the first heating run (Figure 5, left), the processing methods impart their influence on the thermal behavior of the polymer material. These changes are reversible as the normal thermal profile of PSU is regained in the second run. Virgin PSU (Figure 5, C) exhibits a glass transition temperature at 189 °C followed by enthalpic relaxation. When looking at the rotor milled PSU (Figure 5, B). A clear T_g at approx. 189 °C is visible followed by a slight endothermic peak going from 210 °C to 236 °C. The peak, as was the case with ball milling, disappears upon heating above the endotherm and reanalyzing in the second heating run (Figure 5, B) and suggests orientation imposed by the processing method on to the polymer chains. During processing the polymer chains of the material stretch out when the pellets of powder impact on the rotor blades and get further sheared apart between the blades and the sieving ring. Upon the first heating run an endothermic peak is then visible ascribed to the relaxation of the chains. Upon the second run the T_g remains visible and stable indicating no severe degradation occurring in the process.

With spray drying the PSU was first dissolved, then atomized and dried to form spherical particles. Samples were consequently dried for two days in a vacuum oven at 50 °C in order to remove any residual solvent. A clear T_g is visible at 188 °C with two small endothermic peaks at 237 °C and 262 °C in the first heating run (Figure 5, A). These peaks disappear upon heating above their offset temperature and also suggest a form of orientation imposed on to the polymer chains by the processing method through the high shearing rates the polymers experience while jetting into the drying chamber. The second heating curve shows a clear Tg again at 189 °C in accordance with the unprocessed PSU (Figure 5, A).

4 CONCLUSION

Polysulfone and syndiotactic polystyrene were processed into powder form for the use of Selective Laser Sintering. Rotor milling could successfully be used in a three step refinement process to produce particles of desired size (51,8 ± 15,2 µm for PSU and 49,2 ± 15,6 µm for sPS) and morphology. In this regard, the more brittle sPS displayed more irregular structures which was reflected in a higher Hausner ratio. Nevertheless the Hausner Ratio for both rotor milled samples fell within the range of good flowability, which is essential for SLS purposes.

In the case of spray drying particles were prominently spherical yet particle size deemed a bit lacking for PSU (26,1 µm ± 12,8 µm) and was too small for sPS (6,6 ± 6,9 µm). This could be explained by the low solubility of the latter in the chosen solvent.

Both processing methods imparted some orientation in the polymer chains causing extensive enthalpic relaxation visible in the DSC measurements for PSU and amorphization in crystallinity for sPS. Spray drying could offer a good alternative as a physicochemical processing technique yet it requires more optimization in regards to particle size and density.

5 REFERENCES

Athreya, S.R., Kalaitzidou, K. & Das, S., 2010. Processing and characterization of a carbon black-filled electrically conductive Nylon-12 nanocomposite produced by selective laser sintering. *Materials Science and Engineering: A*, 527(10), pp.2637–2642.

Bai, C. et al., 2000. Structural changes in poly (ethylene terephthalate) induced by mechanical milling. , 41, pp.7147–7157.

Bai, J. et al., 2012. Carbon nanotube reinforced Polyamide 12 nanocomposites for laser sintering. *Proceeding of the Solid Freeform Fabrication Symposium*, 7, pp.98–107.

Barbosa-Cánovas, G. V et al., 2005. Bulk properties. *Food Powders: Physical Properties, Processing, and Functionality*, pp.55–90.

Berzins, M., Childs, T.H.C. & Ryder, G.R., 1996. The Selective Laser Sintering of Polycarbonate. *CIRP Annals*, 45(1), pp.187–190. Available at: https://www.sciencedirect.com/science/article/pii/S0007850607630443 [Accessed March 14, 2018].

Bodhmage, A., 2006. Correlation between physical properties and flowability indicators for fine

powders.
Dadbakhsh, S. et al., 2016. Effect of Powder Size and Shape on the SLS Processability and Mechanical Properties of a TPU Elastomer. *Physics Procedia*, 83, pp.971–980. Available at: https://www.sciencedirect.com/science/article/pii/S1875389216302097 [Accessed April 10, 2018].
Drummer, D. et al., 2015. Modelling of the aging behavior of polyamide 12 powder during laser melting process. In *AIP Conference Proceedings*. AIP Publishing, p. 160007.
Drummer, D., Rietzel, D. & Kühnlein, F., 2010. Development of a characterization approach for the sintering behavior of new thermoplastics for selective laser sintering. *Physics Procedia*, 5, pp.533–542.
Goodridge, R.D., Hague, R.J.M. & Tuck, C.J., 2010. Effect of long-term ageing on the tensile properties of a polyamide 12 laser sintering material. *Polymer Testing*, 29(4), pp.483–493.
Goodridge, R.D., Tuck, C.J. & Hague, R.J.M., 2012. Laser sintering of polyamides and other polymers. *Progress in Materials Science*, 57(2), pp.229–267. Available at: http://dx.doi.org/10.1016/j.pmatsci.2011.04.001.
Grabowski, W. & Wilanowicz, J., 2008. The structure of mineral fillers and their stiffening properties in filler-bitumen mastics. *Materials and Structures*, 41(4), pp.793–804.
Ho, H.C.., Gibson, I. & Cheung, W.., 1999. Effects of energy density on morphology and properties of selective laser sintered polycarbonate. *Journal of Materials Processing Technology*, 89–90, pp.204–210. Available at: https://www.sciencedirect.com/science/article/pii/S0924013699000072#FIG1 [Accessed March 14, 2018].
Jonna, S. & Lyons, J., 2005. Processing and properties of cryogenically milled post-consumer mixed plastic waste. *Polymer Testing*, 24(4), pp.428–434. Available at: http://www.sciencedirect.com/science/article/pii/S0142941805000139 [Accessed April 28, 2015].
Kruth, J. et al., 2008. Consolidation of Polymer Powders by Selective Laser Sintering. *International Conference on Polymers and Moulds Innovations*, pp.15–30.
Mys, N., 2017. *Processing and Characterization of Polymeric Materials to Spherical Powders as Candidate Build Material for fusion Based Additive Manufacturing*, Ghent: Ghent University. Available at: https://lib.ugent.be/catalog/rug01:002382526.
Mys, N., Van De Sande, R., et al., 2016. Processing of Polysulfone to Free Flowing Powder by Mechanical Milling and Spray Drying Techniques for Use in Selective Laser Sintering. *Polymers* , 8(4).
Mys, N., Verberckmoes, A. & Cardon, L., 2016. Processing of Syndiotactic Polystyrene to Microspheres for Part Manufacturing through Selective Laser Sintering. *Polymers*, 8(11), p.383.
Pohle, D. et al., 2007. Processing of Three-Dimensional Laser Sintered Polyetheretherketone Composites and Testing of Osteoblast Proliferation in vitro. In *Macromolecular Symposia*. Wiley Online Library, pp. 65–70.
Powers, M.C., 1982. Comparison chart for estimating roundness and sphericity. *AGI data sheet*, 18(1).
Raabe, D., Chen, N. & Chen, L., 2004. Crystallographic texture, amorphization, and recrystallization in rolled and heat treated polyethylene terephthalate (PET). *Polymer*, 45(24), pp.8265–8277.
Schmid, M. et al., 2013. Flowability of Powders for Selective Laser Sintering (SLS) investigated by Round Robin Test. In *High Value Manufacturing: Advanced Research in Virtual and Rapid Prototyping: Proceedings of the 6th International Conference on Advanced Research in Virtual and Rapid Prototyping, Leiria, Portugal, 1-5 October, 2013*. CRC Press, p. 95.
Schmidt, M., Pohle, D. & Rechtenwald, T., 2007. Selective laser sintering of PEEK. *CIRP Annals-Manufacturing Technology*, 56(1), pp.205–208.
Strobbe, D. et al., 2016. Selective laser sintering of polystyrene: a single layer approach.
Tiwari, S.K. et al., 2015. Selection of selective laser sintering materials for different applications. *Rapid Prototyping Journal*, 21(6), pp.630–648.
Vasquez, G.M. et al., 2014. A targeted material selection process for polymers in laser sintering. *Additive Manufacturing*, 1(4), pp.127–138.
Vehring, R., Foss, W.R. & Lechuga-Ballesteros, D., 2007. Particle formation in spray drying. *Journal of Aerosol Science*, 38(7), pp.728–746.
Wegner, A. et al., 2015. Determination of Optimal Processing Conditions for the Production of Polyamide 11 Parts using the Laser Sintering Process. *International Journal of Recent Contributions from Engineering, Science & IT (iJES)*, 3(1), pp.5–12.
Woo, E.M., Sun, Y.S. & Yang, C.P., 2001. Polymorphism, thermal behavior, and crystal stability in syndiotactic polystyrene vs. its miscible blends. *Progress in Polymer Science (Oxford)*, 26(6), pp.945–983.
Zhou, W. et al., 2013. Melting process and mechanics on laser sintering of single layer polyamide 6 powder. *The International Journal of Advanced Manufacturing Technology*, 69(1–4), pp.901–908.
Ziegelmeier, S. et al., 2015. An experimental study into the effects of bulk and flow behaviour of laser sintering polymer powders on resulting part properties. *Journal of Materials Processing Technology*, 215, pp.239–250. Available at: http://www.sciencedirect.com/science/article/pii/S092401361400288X.
Ziegelmeier, S. et al., Characterizing the Bulk & Flow Behaviour of LS Polymer Powders.